ASSESSMENT OF STRUCTURAL ROBUSTNESS AGAINST AIRCRAFT IMPACT AT THE POTENTIAL REPOSITORY AT YUCCA MOUNTAIN—PROGRESS REPORT II

Prepared for

**U.S. Nuclear Regulatory Commission
Contract NRC–02–02–012**

Prepared by

**P.A. Cox
J. Mathis
T. Wilt
A. Chowdhury
A. Ghosh**

**Center for Nuclear Waste Regulatory Analyses
San Antonio, Texas**

September 2006

Previous Reports in Series

Name	Date Issued
Assessment of Structural Robustness Against Aircraft Impact at the Potential Repository at Yucca Mountain—Progress Report	August 2005

ABSTRACT

The U.S. Department of Energy intends to design the exterior walls of the dry transfer, canister handling, and fuel handling facilities so they could not be penetrated or collapsed by the impact of an F-16 aircraft crashing at the 95th percentile speed based on historical F-16 crashes Ragan (2005). This report is a continuation of the previous work of Cox, et al. (2005) to develop an analysis approach involving (i) refinements of the concrete damage model characterization, (ii) structural modeling of an engine simulant representing a GE J79 aircraft engine, and (iii) evaluation of the Riera method for calculating impact forces. Adjusting the concrete damage model parameters produces only minor, consistent changes in front face penetration, but improves correlation with the wall back surface displacements measured in the full-scale engine model test. The engine simulant model behaves similarly, in terms of load displacement and absorbed energy, to the full-scale idealized engine when subjected to a quasi-static crush test. A comparison with measured test results shows that the Riera method produces a conservative calculation of impact forces, the magnitude of which can be adjusted through the use of a mass adjustment factor described in this report. Finally, using the refinements to the concrete damage model parameters, a reinforced concrete wall is modeled using LS-DYNA. The Riera method presented in this report calculates the impact force on the concrete wall. Preliminary results show that at peak deflection, cracking is likely to occur due to tensile stresses with scabbing and spalling on the rear side of the wall.

REFERENCE

Cox, P.A., J. Mathis, and A. Ghosh. "Assessment of Structural Robustness Against Aircraft Impact At The Potential Repository At Yucca Mountain—Progress Report." San Antonio, Texas: CNWRA. August 2005.

Ragan, G.E. "Frequency Analysis of Aircraft Hazards for License Application." 000–00C–WHS0–00200–000–00C. Las Vegas, Nevada: Office of Civilian Radioactive Waste Management. Department of Energy. May 2005.

CONTENTS

FIGURES

FIGURES

TABLES

ACKNOWLEDGMENTS

QUALITY OF DATA, ANALYSES, AND CODE DEVELOPMENT

DATA: All CNWRA-generated original data contained in this report meet the quality assurance requirements described in the Quality Assurance Manual (Geosciences and Engineering Division, 2005). Data used in this report are primarily experimental observations derived from other publicly available sources. Each data source is cited in this report and should be consulted for determining the level of quality for those cited data. The work presented in this report is documented in Scientific Notebooks 702 and 776.

ANALYSES AND CODES: The finite element analyses presented in this report were conducted using ANSYS™ Version 10.0 (ANSYS, Inc., 2005) which includes LS-DYNA Version Mpp970 (Livermore Software Technology Corporation, 2003). ANSYS Version 10.0 and LS-DYNA Mpp970 are controlled under Technical Operating Procedure–018, Development and Control of Scientific and Engineering Software. Spreadsheet calculations were accomplished using Microsoft® Excel® (Microsoft Corporation, 2002).

References

ANSYS, Inc. "ANSYS." Version 10.0. Canonsburg, Pennsylvania: ANSYS, Inc. 2005.

Geosciences and Engineering Division. "Quality Assurance Manual" San Antonio, Texas: CNWRA. 2005.

Livermore Software Technology Corporation. "LS-DYNA User's Manual." Version 970. Livermore, California: Livermore Software Technology Corporation. April 2003.

Microsoft Corporation. "Microsoft® Excel® 2002.5P3." Redmond, Washington: Microsoft Corporation. 2002.

1 INTRODUCTION

1.1 Background

Agreement PRE.3.01 (Reamer and Gil, 2001) was made between U.S. Nuclear Regulatory Commission (NRC) and U.S. Department of Energy (DOE) in the technical exchange and management meeting on July 24–26, 2001. By this agreement, the DOE agreed to collect information for civilian and military aircraft flight activities in the vicinity of the site that may pose a hazard to the proposed geologic repository operations area (GROA) surface facilities. In addition, DOE agreed to perform analyses to estimate the annual frequency of aircraft crash hazards. The DOE prepared two reports (Morissette and Ziegler, 2002; Ragan, 2003) as a response to this agreement. NRC and DOE engaged in two additional technical exchanges on September 20, 2003 and June 1, 2005, on aircraft crash hazard analysis. Discussions in the technical exchange on June 1, 2005, were based on Ashley (2005) and Ragan (2005a). In Ragan (2005a), credit for robustness for important to safety structures was taken to reduce the annual frequency of aircraft crashes onto surface facilities at the potential repository at Yucca Mountain. Based on the discussions at this technical exchange and information presented in Ashley (2005) and Ragan (2005a), NRC considered the agreement PRE.3.01 closed because DOE provided a plan for identification and estimation of aircraft hazards for the potential license application. However, some issues remain, including the bases for taking credit for structural robustness to withstand the impact from an F-16 aircraft crashing at the 95 percentile speed estimated from historical F-16 crashes. Also in question was the suitability of the DOE methodology for assessing the structural robustness of engineered barriers in an aircraft crash. Staff informed DOE about 13 high-level issues in a letter dated August 2, 2005 (Kokajko, 2005).

10 CFR 63.112(e)(8) requires that DOE should analyze the performance of safety structures that are relied on to limit or prevent progression of potential event sequences. In Ragan (2005a), DOE asserted that the robustness of the walls of the surface facilities and the barrier wall of the aging facility would limit or prevent progression of any event sequences initiated by a crashing aircraft with an impact speed corresponding to the 95th percentile of the probability distribution estimated from historical F-16 crashes only. DOE also proposed to submit calculations to substantiate the credit taken for structural robustness. Therefore, in response, staff initiated a study to develop staff capabilities to review future DOE analyses of aircraft impacting an important to safety structures and, if needed, to conduct our own confirmatory analyses. A report (Cox, et al., 2005) documented the progress made in developing the necessary expertise to review aircraft impact analyses in fiscal year 2005. Staff plans to conduct the actual impact analysis of a crashing aircraft under safeguard restrictions using a secure computer system with appropriate computing capabilities. The computer system has been installed in a designated secured room. Center for Nuclear Waste Regulatory Analyses (CNWRA) is currently waiting for NRC to certify the security arrangements in this room to start the safeguarded portion of this study.

In the meantime, DOE revised the report (Ragan, 2005a) and published a second study (Ragan, 2005b), where no credit for structural robustness of the structures, systems, and components important to safety was taken. However, significant changes to the analysis were proposed. DOE has abandoned the possibility of developing a Memorandum of Understanding with the United States Air Force to implement a no-fly zone. Instead, the DOE approach is to formally inform the United States Air Force of the future flight restrictions. It has been assumed in the analysis presented in Ragan (2005b) that the pilots would be aware of the flight restrictions and

follow them in emergencies, thereby reducing the annual frequency of aircraft crashes. The estimated annual frequency of aircraft crashes at the potential Geologic Repository Operations Area surface facilities in Ragan (2005b) is 1.6×10^{-6}. The uncertainties associated with the data and analysis presented (e.g., pilot avoidance, aircraft and flight information and their flight characteristics in the vicinity of the surface facilities, etc.) warrant exploring the consequences of an aircraft crash into important to safety structures.

Staff will review, if necessary, DOE analyses in the license application on robustness of structures to withstand a potential aircraft crash and continue the safety functions assigned, thereby limiting or preventing potential event sequences. Additionally, staff should be able to independently verify DOE assessments of robustness of different structures.

1.2   Objectives and Scope

As mentioned above, the staff needs to develop the capability to review DOE analyses in the license application by independently modeling the phenomena associated with intense impact loading imparted by a crashing aircraft on reinforced concrete structures. This will allow staff to review and independently verify DOE assessments of the structural robustness of specific structures to withstand aircraft crashes.

This review will involve the adequacy of the modeling approach, the selection of parameters to characterize the response of reinforced concrete structures under impact loading, and the methods of computing loads on structures imparted by an aircraft crash.

This report addresses the ability of the LS-DYNA concrete damage model to accurately predict the displacements from a full-scale F-4 engine simulant impacting a concrete wall, as presented by Muto, et al. (1989). Comparing the numerical simulation results with experimental observations assists in selecting the appropriate concrete damage material parameters and establishes a methodology to determine the values for the model parameters. Additionally, this report investigates the accuracy of the Riera method for computing the loads imparted to a rigid surface by an aircraft crash. This method calculates the impact force on a target concrete block and measures and compares the displacement and velocity of the block to test data. Using the Riera method, a preliminary analysis evaluates the impact damage produced by the F-4 aircraft on a reinforced concrete wall.

The scope of this work is divided into four parts. The first is a finite element, quasi-static analysis of an idealized engine simulant, constructed of steel, that represents a GE J79 engine. Analyses are performed to allow adjustment in the plastic material parameters of the steel to match the load displacement and energy absorption of the full-scale engine simulant. Second, the material parameters associated with the concrete damage model are adjusted to improve the calculated displacement response of the target wall. This concrete damage parameter adjustment is performed so that it does not significantly affect previous calculations (Cox, et al., 2005) of front face penetration of the target wall. Third, the use of the Riera method to calculate impact loads is compared with measured test data to assess the method's accuracy. The fourth part of this study is the application of the calculated load-time history using the Riera method and the new concrete damage model material parameters for the preliminary analysis of a reinforced concrete wall.

2 REFINEMENTS IN CONCRETE DAMAGE MODEL MATERIAL PARAMETERS

Results from the materials characterization study for the concrete damage model were presented in the last progress report (Cox, et al., 2005). In that report, the concrete damage model in LS-DYNA (Livermore Software Technology Corporation, 2003) was determined to be the most appropriate since it had been successfully used for modeling concrete structures (Malvar, et al., 1997). The material parameters selected in the last progress report were found to give good quantitative results, in terms of peak back surface displacements, when compared to experiments on reinforced concrete walls loaded by pressure generated from detonation of high explosives and by impact from simulated aircraft engines.

Although the peak displacements were comparable (Cox, et al., 2005), the characteristic feature of bounce back, as observed in experiments (Malvar, et al., 1997), was not reproduced using the concrete material parameters previously reported in Cox, et al. (2005). To more accurately model the impact response of concrete structures, additional refinements to the concrete damage material parameters were deemed necessary to improve correlation with the full-scale impact test as reported by Muto, et al. (1989) and Esashi, et al. (1989). Numerical modeling of this full-scale test requires accurate structural behavior of the engine simulant representing the GE J79 engine, as well as the concrete damage model's material parameters.

2.1   Engine Simulant

The first step of this study focused on the behavior of the engine simulant. A full-scale impact test was conducted with an idealized model of the GE J79 engine used in the F-4 fighter (Muto, et al.,1989). Figure 2-1 shows the relative dimensions of the simplified model used in this report. To correctly model the full-scale impact event, it was necessary to first determine whether the engine simulant model was exhibiting the proper crush performance under a controlled loading condition. Therefore, a comparison of modeling results with static compression tests of the engine simulant used in the full-scale impact experiment was completed. The known material data representing steel is the yield strength of 349.1 MPa [50.6 ksi], an ultimate strength of 687.4 MPa [99.7 ksi], and a Young's modulus of 201,000 MPa [29,145 ksi] (Muto, et al., 1989). With this information, an elastic-plastic with kinematic hardening material model, specified by the keyword *MAT_PLASTIC_KINEMATIC in LS-DYNA, was used in the analysis. The elastic–plastic material model, which accounts for strain-hardening effects, uses a bilinear approximation for the material stress-strain relationship and is based on user input of yield strength, ultimate strength, Young's modulus, tangent modulus (hardening slope), and Poisson's ratio. This model also accounts for strain rate dependence through the use of the Cowper-Symonds modification which scales the yield stress σ_y by a factor which depends on the strain rate $\dot{\varepsilon}$ i.e.,

$$\sigma_y = \sigma_y \left[1 + \left(\frac{\dot{\varepsilon}}{C} \right)^{\frac{1}{p}} \right] \tag{2-1}$$

GE J79 Engine

GE J79 Engine Simulant
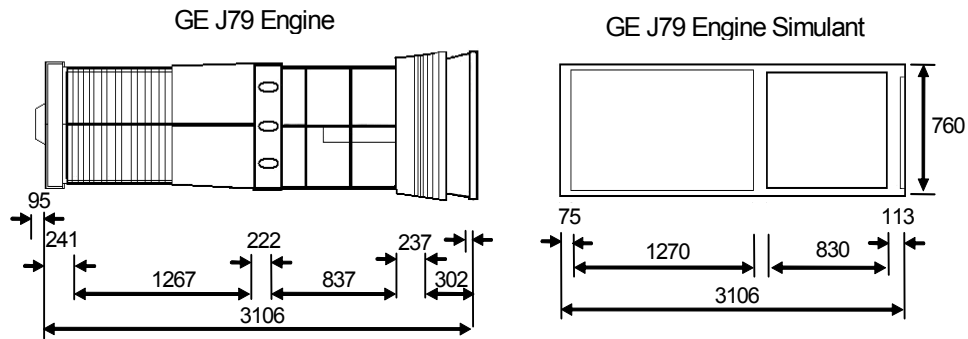
Figure 2-1. Idealized Engine Model of GE J79 Engine Used in Finite Element Simulation of Full-Scale Test Performed by Muto, et al. (1989) (All Dimensions Are Given in mm) [25.4 mm = 1 in]

where C and p are material parameters. The values of all necessary material parameters defined above are given in Table 2-1.

The loading of the full-scale engine simulant was applied during the test via a displacement-controlled hydraulic ram in which the rate of compression was 2 m/s [6.56 ft/s]. Similarly, the finite element model used a displacement-controlled boundary condition to crush the engine simulant, and the resultant compression force was tracked using the keyword ∗RIGIDWALL option in LS-DYNA. The rigid wall option provides the ability to treat contact between a rigid surface and nodal points on a deformable body. The nodal points are defined as slave nodes. In this application, the rigid wall is defined at the bottom of the engine simulant, and the force is measured there. The top of the engine simulant has the specified displacement boundary conditions. The progressive crushing of the engine simulant is shown in Figure 2-2. The load-displacement results of the crushing simulation were compared with experimental test data as shown in Figure 2-3. Good agreement is observed overall, with the average load between zero and 1 m [3.28 ft] of displacement matching the test data very well.

Table 2-1. List of Elastic–Plastic Material Parameters	
Poisson's Ratio	0.3
Yield Strength, MPa [ksi]	349.1 [50.6]
Young's Modulus, MPa [ksi]	201,000 [29,145]
Tangent Modulus, MPa [ksi]	8,500 [1,233]
Cowper-Symonds, c 1/sec	40
Cowper-Symonds, p	5
Failure Strain	0.8

Figure 2-2. Displacement-Controlled Finite Element Simulation of Progressive Crushing of the Engine Simulant (t in Seconds)

Figure 2-3. Load Versus Displacement From Progressive Crushing of Engine Simulant: Comparison of LS-DYNA Results and Test Data of Muto, et al. (1989) [1 m = 3.28 ft; 1 N = 0.225 Lbf]

It is not until the projectile is crushed down to the stiffer lower section that the numerical simulation results start to differ from the test. The absorbed energy predicted by the numerical simulation als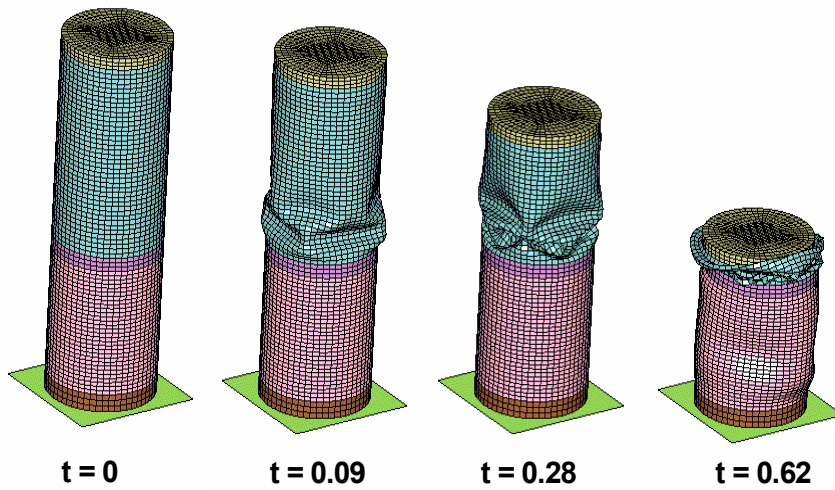o compared well with test data as shown in Figure 2-4. These results show that the engine simulant finite element model behaves similarly to the actual idealized engine used in the quasi-static crush test.

Additional data available from the full-scale impact test was the post test condition of the engine simulant projectile. The test showed that the projectile crushed up to the middle bulkhead and the thicker aft section broke into large pieces. The simulation showed the projectile was crushed to the middle bulkhead; however, the model did not predict fracture of the aft section. Figure 2-5 shows the condition of the crushed projectile after the simulation was complete. Note that the crush rate will affect the rate-dependent material response (i.e., a lower crush rate will result in a softer material response). Future work may involve additional test data performed at different rates to more accurately characterize the material (i.e., the Cowper-Symonds parameters).

2.2   Concrete Material Parameters

The concrete damage model, used to characterize reinforced concrete, is a three-invariant (i.e., pressure dependency is included) plasticity model that accounts for changes in yield stress through the use of a damage function as defined in the LS-DYNA Keyword Users Manual (Livermore Software Technology Corporation, 2003). A brief description of the concrete damage model is given here to define the various material parameters given in subsequent tables. The deviatoric stress is limited by the function $\Delta\sigma_{(y,m,r)}$ defined by linear relationships of
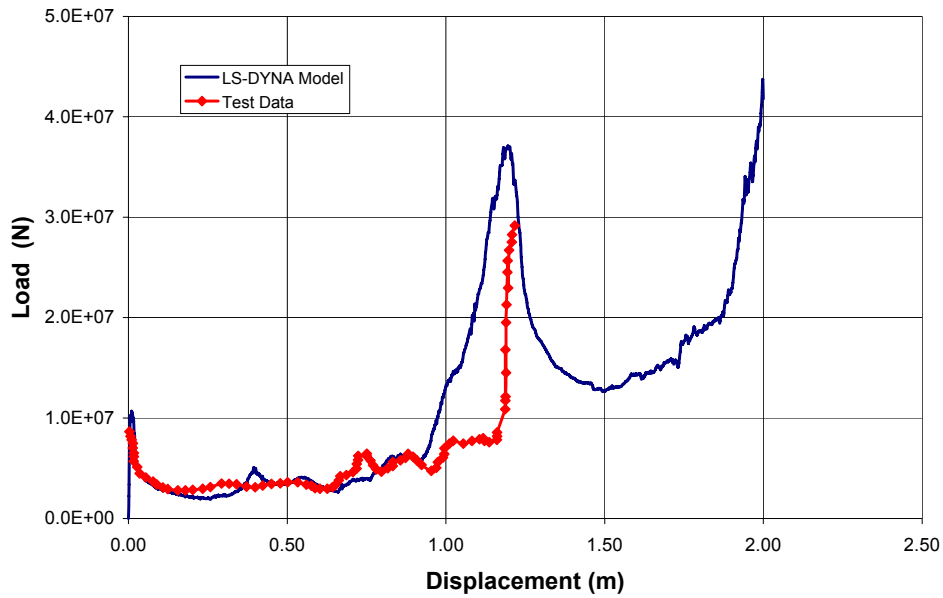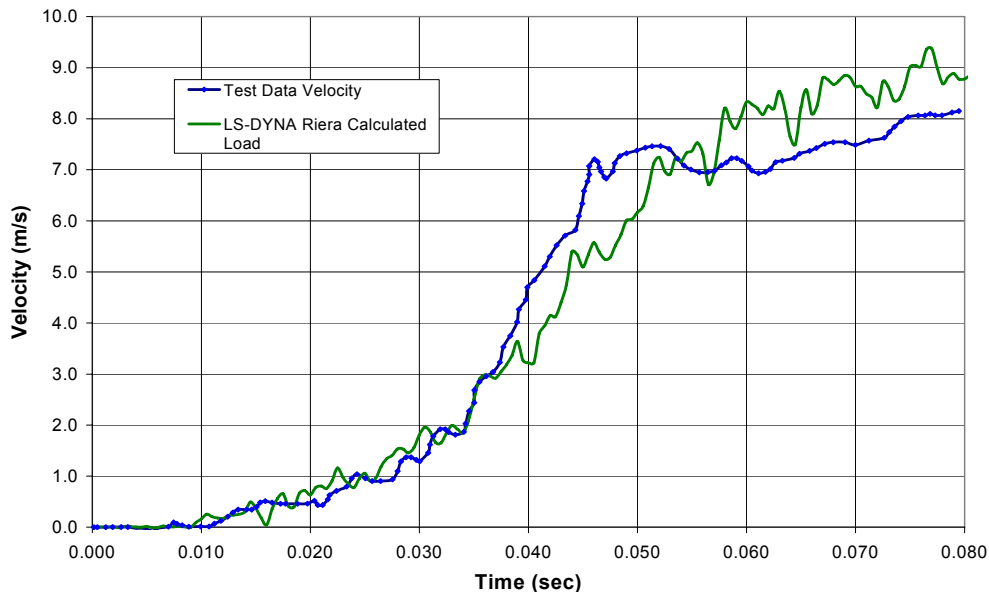

Figure 2-4. Absorbed Energy Versus Time for Progressive Crushing of Engine Simulant: Comparison of LS-DYNA Results and Test Data of Muto, et al. (1989) [1 m = 3.28 ft; IN m = 0.738 Lbf ft]
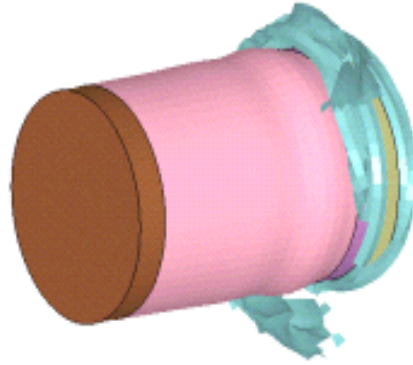
Figure 2-5. Crushed Engine Simulant Model at Completion of Displacement-Controlled LS-DYNA Finite Element Simulation

three failure surfaces that are functions of pressure: (i) initial yield surface, (ii) maximum failure surface, and (iii) residual failure surface, i.e.,

$$\Delta\sigma_y = a_{0Y} + \frac{P}{a_{1Y} + a_{2Y}P} \qquad \text{(Initial yield surface)} \qquad (2\text{-}2)$$

$$\Delta\sigma_m = a_0 + \frac{P}{a_1 + a_2P} \qquad \text{(Maximum failure surface)} \qquad (2\text{-}3)$$

$$\Delta\sigma_r = \frac{P}{a_{1f} + a_{2f}P} \qquad \text{(Residual failure surface)} \qquad (2\text{-}4)$$

in which P is pressure. The yield surface, as is normally defined in standard plasticity, determines the stress state at which plasticity first occurs. Then the yield surface increases to the maximum failure surface, which defines the upper limit on the stress. Past this limit, the material begins to soften until the residual failure surface is reached. Note that the above surfaces are defined by eight material parameters: $a_{0Y}, a_{1Y}, a_{2Y}, a_0, a_1, a_2, a_{1f}, a_{2f}$.

To define the current failure surface, an interpolation is made between the two active failure surfaces. That is, after reaching the yield surface, yet below the maximum surface, the current yield surface is defined as

$$\Delta\sigma = \eta\left(\Delta\sigma_m - \Delta\sigma_y\right) + \Delta\sigma_y \qquad (2\text{-}5)$$

Once the maximum failure surface has been reached, the material begins to soften, and the stress is now interpolated between the maximum failure surface and the residual failure surface, i.e.,

$$\Delta\sigma = \eta\left(\Delta\sigma_m - \Delta\sigma_r\right) + \Delta\sigma_r \qquad (2\text{-}6)$$

The variable η introduced in the above expressions is the damage function, defined by the user in terms of (η, λ) pairs where the term λ is the accumulated effective plastic strain. The damage function is intended to start at zero, increase to a value of one which represents the concrete's maximum strength, and then decrease (i.e., soften) to a value of zero which corresponds to the concrete's residual strength. The values for the damage function $\eta(\lambda)$ are given in Table 2-2. These values were suggested in the LS-DYNA Keyword User's Manual (Livermore Software Technology Corporation, 2003).

Table 2-2. Damage Function in the Concrete Damage Model	
Effective Plastic Strain	**Damage Scale Factor**
λ	$\eta(\lambda)$
0	0.309
8.62×10^{-6}	0.543
2.15×10^{-5}	0.84
3.14×10^{-5}	0.975
3.95×10^{-4}	1.0
5.17×10^{-4}	0.79
6.38×10^{-4}	0.63
7.98×10^{-4}	0.469
9.67×10^{-4}	0.383
1.41×10^{-3}	0.247
1.97×10^{-3}	0.173
2.59×10^{-3}	0.136
0.909	0

Material parameters used in the concrete damage model and reported by Cox, et al. (2005) are listed in Table 2-3. Most of the parameters in Table 2-3 are well defined in the LS-DYNA Keyword User's Manual (2003) or by Malvar, et al. (1997).

The accumulated damage in the present concrete model can be separated into deviatoric and volumetric components. First, consider the case of shear (deviatoric) damage accumulation. For the case of the current failure surface being interpolated between the maximum failure surface and either the yield or residual surfaces, the value for the modified effective plastic strain λ may be defined as:

$$\lambda = \begin{cases} \int \dfrac{d\bar{\varepsilon}^p}{(1+p/f_t)^{b_1}} & \text{for} \quad p \geq 0 \\[4mm] \int \dfrac{d\bar{\varepsilon}^p}{(1+p/f_t)^{b_2}} & \text{for} \quad p < 0 \end{cases} \qquad (2\text{-}7)$$

where p is pressure and b_1 and b_2 are material parameters. Note that when the pressure equals zero, the damage will continuously evolve and will be different for tension and compression.

Now consider the case of volumetric damage that occurs for a pure triaxial test (i.e., no deviatoric component). Once the pressure equals $-f_t$, the effective plastic strain will not evolve. Therefore, in order to allow the damage to continue to evolve, a volumetric damage component is added. Specifically, the increment in effective plastic strain is given by

$$\Delta\lambda = b_3 f_d k_d (\varepsilon_v - \varepsilon_v^{\text{yield}}) \qquad (2\text{-}8)$$

where b_3 is an input scalar multiplier, f_d and k_d are internally calculated scalar multipliers, ε_v is the volumetric strain, and $\varepsilon_v^{\text{yield}}$ is the volumetric strain at yield. The parameter b_1 governs softening in compression, while the parameters b_2 and b_3 govern the softening in the unconfined uniaxial tension stress-strain curve and the triaxial tensile stress-strain curve, respectively. Normally, these parameters are adjusted to match stress-strain test data for a particular concrete.

Because only the concrete compressive strength f_c' was provided in Muto, et al. (1989), there was insufficient experimental information upon which to base the parameters b_1, b_2, and b_3. The b_1 parameter was taken from recommendations in the LS-DYNA Keyword User's Manual (Livermore Software Technology Corporation, 2003), while the concrete parameters b_2 and b_3 were chosen to be modified in order to improve the correlation with the full-scale experimental data (Section 2.2). One additional parameter a_{oY} (cohesion for yield) was modified to better match the suggested yield failure surface curve found in Malvar, et al. (1997).

Table 2-3. Input Material Parameters for the Concrete Damage Model	
Material Parameter	
ρ, kg/m^3 [lb/ft^3] Mass Density	2,300 [144][†]
v Poisson's Ratio	0.19[‡]
f_c', Pa [psi] Compressive Strength of Concrete	2.35×10^7 [3,408][†]
a_0, Pa [psi] Cohesion	5.88×10^6 [853][§]
a_1 Pressure Hardening Coefficient	0.333[§]
a_2 Pressure Hardening Coefficient	1.42×10^{-8}[§]
a_{0Y}, Pa [psi] Cohesion for Yield	2.64×10^6 [383][*]
a_{1Y} Pressure Hardening Coefficient for Yield Limit	0.75[*]
a_{2Y} Pressure Hardening Coefficient for Yield Limit	3.10×10^{-8}[*]
a_{1F} Pressure Hardening Coefficient for Failure	0.39[§]
a_{2F} Pressure Hardening Coefficient for Failure	1.39×10^{-8}[*]
b_1 Damage Scaling Factor	1.250[§]
b_2 Damage Scaling Factor for Uniaxial Tension	4.0[*]
b_3 Damage Scaling Factor for Triaxial Tension	10.0[*]

[*]Malvar, L.J., J. Crawford, J. Wesevich, and D. Simons. "A Plasticity Concrete Material Model for DYNA3D." Int. J. Impact Enginering. Vol. 19, Nos 9–10. pp. 847–873. 1997.
[†]Wang, C.K. and C.G. Salmon. "Reinforced Concrete Design." Fifth Edition. New York, New York: Harper-Collins. 1992.
[‡]MacGregor, J.G. and H.K. Wright. "Reinformed Concrete Mechanics and Design." Fourth Edition. Prentice Hall. 2005.
[§]Livermore Software Technology Corporation. "LS-DYNA Keyword User's Manual." Version 970. Livermore, California: Livermore Software Technology Corporation. April 2003.

2.3   Revisiting the Full-Scale Idealized Engine Impact Analysis

The full-scale test of Muto, et al. (1989) involved a 7-m [23-ft] square and 160-cm [63-in] thick reinforced concrete wall. The concrete compressive strength was 23.5 MPa [3.4 ksi]. The reinforcement ratio was 0.4 percent with reinforcement bars in each face and in both directions. Each reinforcement bar had a diameter of 32 mm [1.3 in] with a 488.7 MPa [71 ksi] yield strength and an ultimate strength of 744 MPa [108 ksi]. The idealized engine had a total mass of 1,463 kg [3,225 lb] and was constructed of steel having a yield strength of 349.1 MPa [50.6 ksi] and an ultimate strength of 687 MPa [99.6 ksi]. The impact speed in the test of the simulated engine missile was 215 m/s [705 ft/s]. The finite element model of the wall consisted of 191,556 eight-noded solid single point integration elements and 14,280 beam elements representing the reinforcement bar. For the solid elements, a Flanagan-Belytschko viscous form with exact volume integration hourglass control was used (Flanagan and Belytschko, 1981). Nodal constraints were applied to a set of nodes in a square pattern 0.75m × 0.75m [2.45 ft × 2.46 ft] at each of the four corners on the backside of the wall. The constraint was in the direction of loading.

Comparisons of back surface displacements, located at the center of the panel on the backside, as reported previously in Cox, et al. (2005) are shown in Figure 2-6. The previous simulations (Cox, et al., 2005) matched measured maximum displacements in magnitude (Figure 2-6) but not in the character of the displacement history. Numerical calculations gave a front face penetration of 22 cm [8.7 in] and no back surface scabbing. The full-scale test produced a front face penetration of 21 cm [8.3 in] with no observed scabbing of the back surface.

As discussed in the previous section of this report, a sensitivity study of the concrete damage parameters b_2 and b_3 was performed in order to improve the match with the experiment. The back surface displacement history for select trial runs is shown in Figure 2-7. The analysis with b_2 = 15 and b_3 = 5 was considered the best fit to the measured data because it exhibited the same trend as the experiment in the latter part of the test, that is, the simulation results now captures the bounce-back effect. The concrete damage model parameters in Table 2-3 remain the same with the exception that b_2 = 15 and b_3 = 5.

Because the offset in the calculated displacements, which begins at about 4 ms, are not evident in the measured displacements, the tangent (hardening) modulus and failure strain material parameters of the engine simulant model were varied (from those listed in Table 2-1) to see the effect on the calculated displacements. From these simulations it became clear that the offset was caused by the collapse of the front cylinder in the engine model. This produced a decrease in the displacement (i.e. penetration slowed) between approximately 4–8 ms and displacement rate resumed when the intermediate bulkhead impacted the wall after full collapse of the front cylinder. Even though modifying the concrete material parameters produced the desired bounce-back in the displacement it did not produce a better fit to measured data and did not eliminate the temporary decrease in the displacement rate observed in the calculations but not in the experimental data.
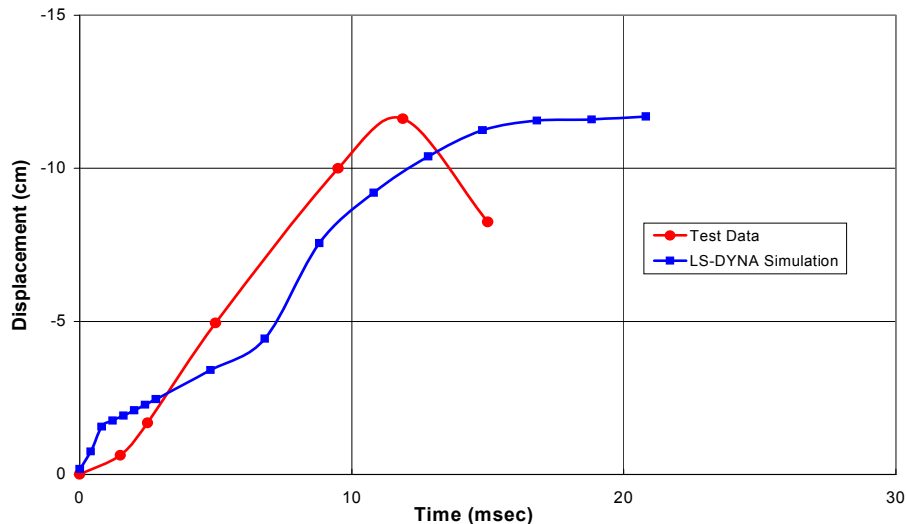

Figure 2-6. Displacement Versus Time Comparison for Full-Scale Panel Test (Muto, et al., 1989) Based on Initial Values of Concrete Damage Model Parameters. Displacement Measured on Backside of Test Panel. [1 cm = 0.39 in]
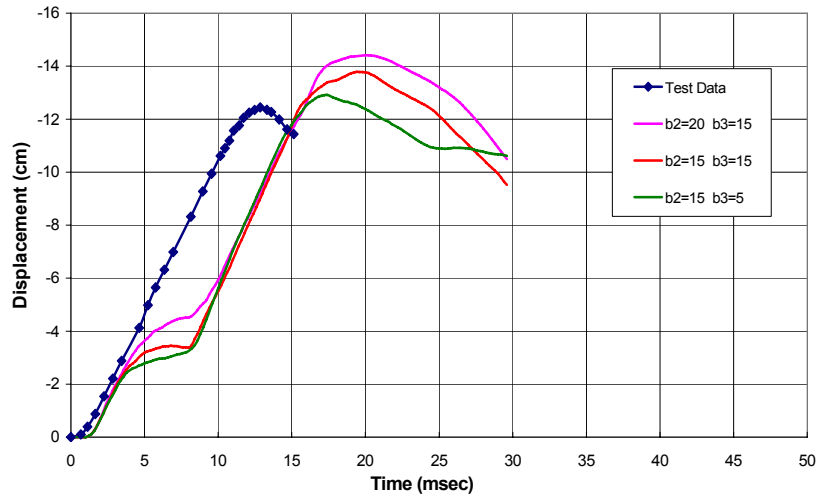
Figure 2-7. Displacement Versus Time Results For Full-Scale Panel Test of Muto, et al. (1989). Trial Runs with Various Values of Concrete Damage Parameters b_2 and b_3. [1 cm = 0.39 in]

The maximum predicted penetration depth also was compared with test results to investigate changes in b_2 and b_3. Recall that the experimental test indicated 21 cm [8.25 in] of penetration into the front face of the concrete wall. The numerical simulation showed a crater depth of approximately 20 cm [7.8 in], which was in good agreement with the test data. A cross-sectional view of the wall is shown in Figure 2-8. This is a change from 22 cm [8.7 in] previously reported in Cox, et al. (2005). Based on the results presented above, there appears to be a coupling between the concrete material parameters and the structural (crush) behavior of the engine simulant, and the structural response of the wall is affected. Additional numerical studies need to be performed to determine the cause of the temporary decrease in the displacement rate which is now present.

20 cm
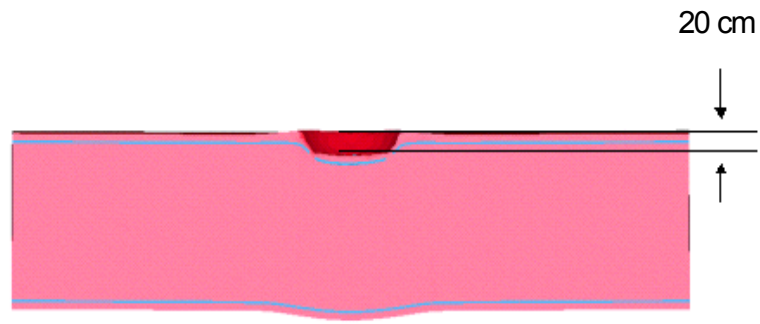
**Figure 2-8. LS-DYNA Finite Element Results Showing Crater Depth Due to Impact of Engine Simulant on Test Panel. Test Indicates 21 cm Crater Depth (Muto, et al., 1989)
[1 cm = 0.39 in]**

3 AIRCRAFT IMPACT LOADS BASED ON THE RIERA METHOD

Currently, DOE has selected F-16s as the aircraft to be used in impact analyses; however, other types of military aircraft may fly in the immediate vicinity of the surface facilities of the potential repository (Ashley, 2005). These aircraft include F-15s, A-10s, newer aircraft, such as F-22s, which may also fly close to the surface facilities of the potential repository when deployed. These aircraft have different weights due to differences in configuration. It is uncertain which aircraft DOE will select as the most critical for structural robustness assessment. The damage potential of a crashing aircraft depends on the combination of the mass of the aircraft (or any hard components, such as engine, landing gear, etc.) and the speed of the impact. The critical impact speed is different for each aircraft type due to differences in the distribution of mass. Therefore, a method to calculate the equivalent impact forces for different types of aircraft is required.

Riera (1968) proposed a numerical method for calculating the dynamic loads of an aircraft that crashes into fixed, rigid surfaces. This method was used in this report to predict loads for the F-4 aircraft. Full-scale experiments have been performed in which the F-4 aircraft was crashed into a massive concrete block. Results of the test, plus the mass distribution and crushing force for the F-4 aircraft, were reported by Sugano, et al. (1993). Additionally, Sugano, et al. (1993) reported the corresponding measured impact forces generated by the F-4 aircraft during the test. These impact forces will be compared to numerical calculations of impact forces using the Riera method (Riera, 1968). Use of the Riera method provides staff with the flexibility to analyze DOE's choice of aircraft.

Using the Riera method and data for the F-4 aircraft, preliminary impact studies were performed for the fuel handling facility (Section 5). The F-4 is similar in size to the F-16 and is expected to cause similar damage. Once the requisite data is available for the F-16 (mass distribution and crush strength), the Riera method can be applied in future studies to calculate the impact forces for this aircraft as well.

3.1 Riera Method

The Riera method (Riera, 1968) is used to calculate the force that results from an impact on a structure using two key assumptions: (i) that the projectile is separated into crushed and uncrushed segments and (ii) that the buckling of the crushed segment acts to decelerate the projectile. According to Riera, the impact force F produced by a crashing aircraft striking a target, normal to the impact surface, at a time t is given by

$$F(t) = P_c[x(t)] + \mu[x(t)]V^2(t) \qquad (3\text{-}1)$$

where $x(t)$, is the distance from the nose of the aircraft, P_c is the load necessary to deform or crush the aircraft, μ is the mass per unit length of the aircraft, and V is the velocity of the uncrushed portion. Both P_c and μ are functions of the position along the aircraft, usually measured from the nose, and $V(t)$ is a function of time. When the distributions of both P_c and μ, as well as the initial impact velocity, are known, Eq. (3-1) can be solved stepwise in time, starting at the instant of impact, to provide the impact force on a rigid surface as a function of time.

3.2   Comparison of Measured and Calculated Impact Forces For the F-4 Full-Scale Crash Test

The mass per unit length μ and crush force P_c were digitized from data reported by Sugano, et al. (1993) and are shown in Figures 3-1 and 3-2, respectively. Position along the length of the aircraft is measured from nose to tail, and μ in Figure 3-1 is given for the basic F-4 aircraft, as well as for the F-4 aircraft in its test configuration with skids and rockets added. The crush force in Figure 3-2 with respect to position along the aircraft was measured during the test and presented by Sugano, et al. (1993). Using this data, an Excel (Microsoft, 2002) spreadsheet program was written to calculate the impact forces shown in Figure 3-3 for the F-4 aircraft. Based on a velocity of 215 m/s [705 ft/s], a comparison between measured impact forces reported by Sugano, et al. (1993) and those calculated by the Riera method (Riera, 1968) are shown in Figure 3-4. Except for a slight time shift, the impact forces are in excellent agreement, with the calculated maximum impact force being only 2.6 percent higher than the maximum measured force. Because the mass per unit length and impact forces (Figures 3-1 and 3-2) reported by Sugano, et al. (1993) are essentially zero for a distance of 1.6 m [4.8 ft] from the nose of the aircraft, the calculated impact forces will be essentially zero in this region. This causes the apparent time shift observed in Figure 3-4. To further compare measured and calculated loads from the aircraft impact, the impact forces in Figure 3-4 were integrated to obtain the total impulse delivered to the rigid surface (Figure 3-5). This comparison shows that the total impulse was overestimated by 22.2 percent using the Riera method.

Adjustments to the mass of the aircraft have been suggested to reduce the forces calculated by the Riera method. Sugano, et al. (1993) showed that uniformly reducing the aircraft mass per unit length μ by a factor of 0.9 produces the best fit to measured data; however, based on Figure 3-5, the data matches very well until about 0.05 seconds into the impact event. Therefore, rather than reduce the mass uniformly along the length of the aircraft, a mass adjustment factor that reduces the mass near the tail of the aircraft seems more suitable. This mass adjustment factor, specific to this case, is shown versus the nondimensional length (x/L) of the aircraft in Figure 3-6. When applied to the calculations using the Riera method, the impulse is reduced to within 10 percent of the measured value as shown in Figure 3-7. The calculated force, using a mass adjustment factor, is now slightly lower in peak magnitude than the measured force (Figure 3-8). Many other adjustments can be made to alter the total impulse. For example, if the mass per unit length of the aircraft is further uniformly reduced to 94 percent of its value (i.e., 0.94 × mass adjustment factor), the calculated total impulse agrees with the measurement, although the peak force is further reduced.

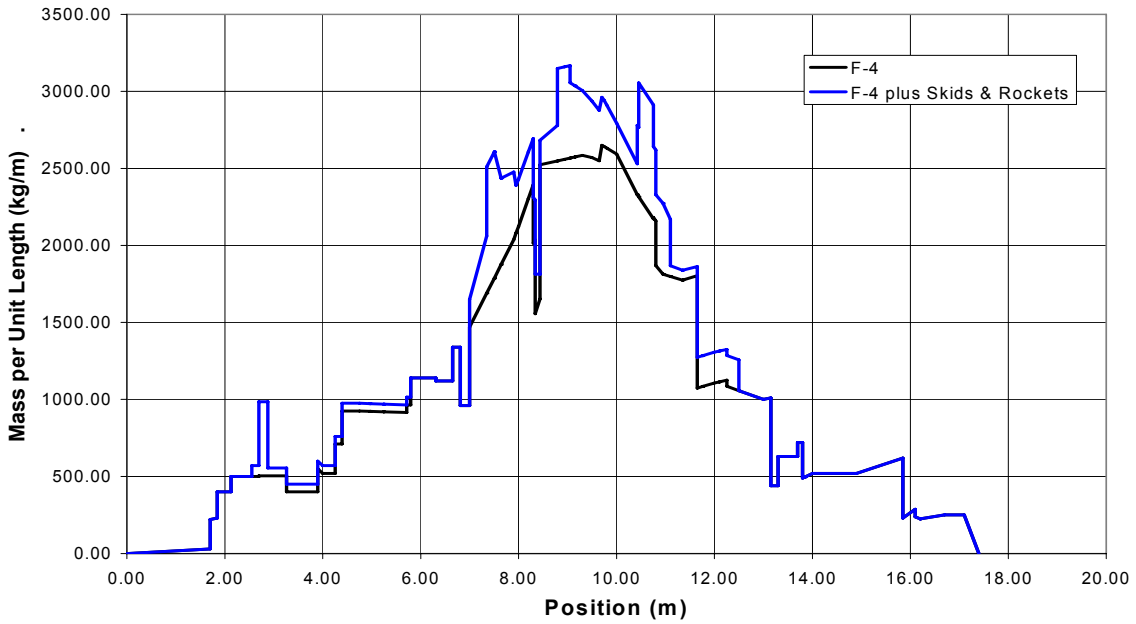**Figure 3-1. Mass per Unit Length, μ, for the F-4 Aircraft With and Without Skids and Rockets Using Digitized Data From Sugano, et al. (1993) [1 kg = 2.2 lb; 1 m = 3.28 ft]**
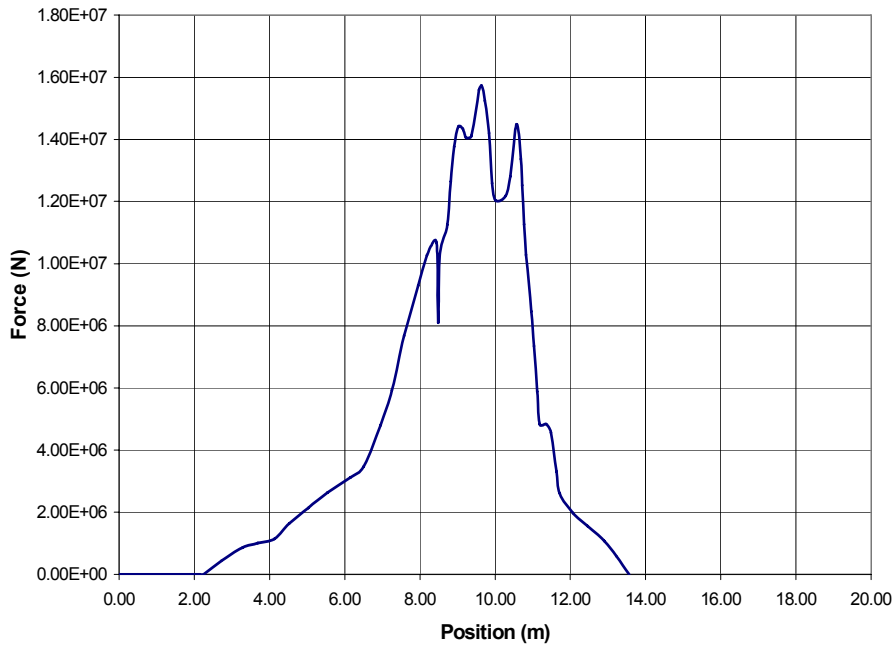

Figure 3-2. Measured Crush Force P_c for the F-4 Aircraft Including Skids and Rockets Using Digitized Data From Sugano, et al. (1993) [1 N = 0.225 Lbf; 1 m = 3.28 ft]
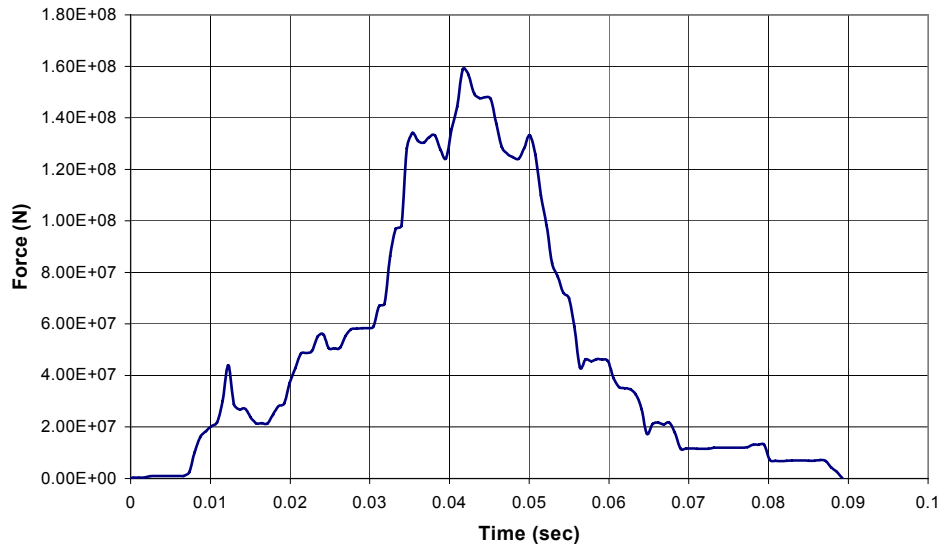
Figure 3-3. Calculated Impact Force on a Rigid Surface Using Riera Method (Riera, 1968) at a Speed of 215 m/s [1 N = 0.225 Lbf]
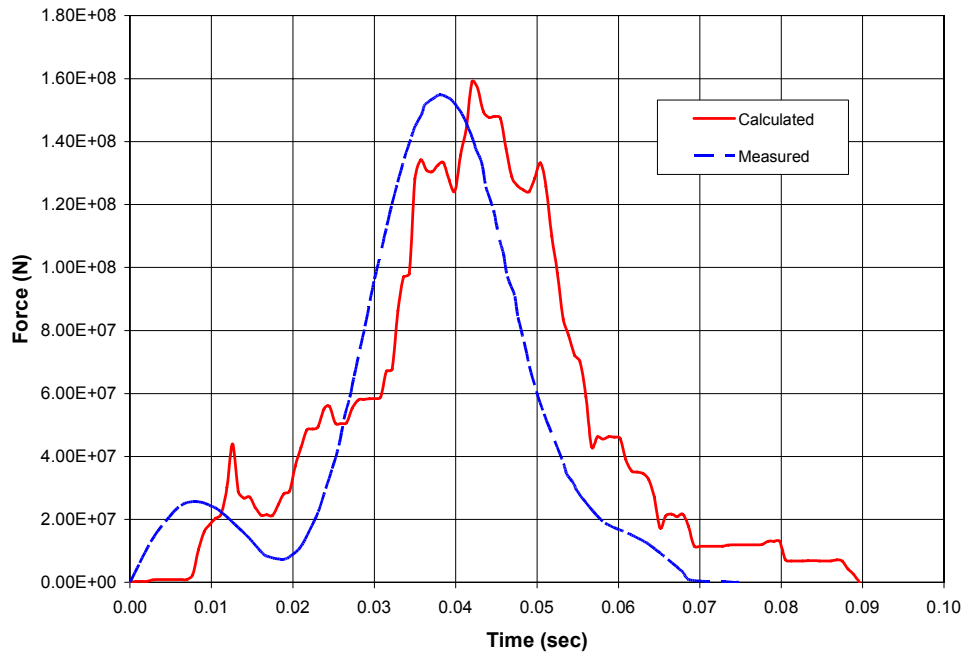

Figure 3-4. Comparison of Measured (Sugano, et al., 1993) and Calculated Impact Forces for the F-4 Aircraft Including Skids and Rockets [1 N = 0.225 Lbf]
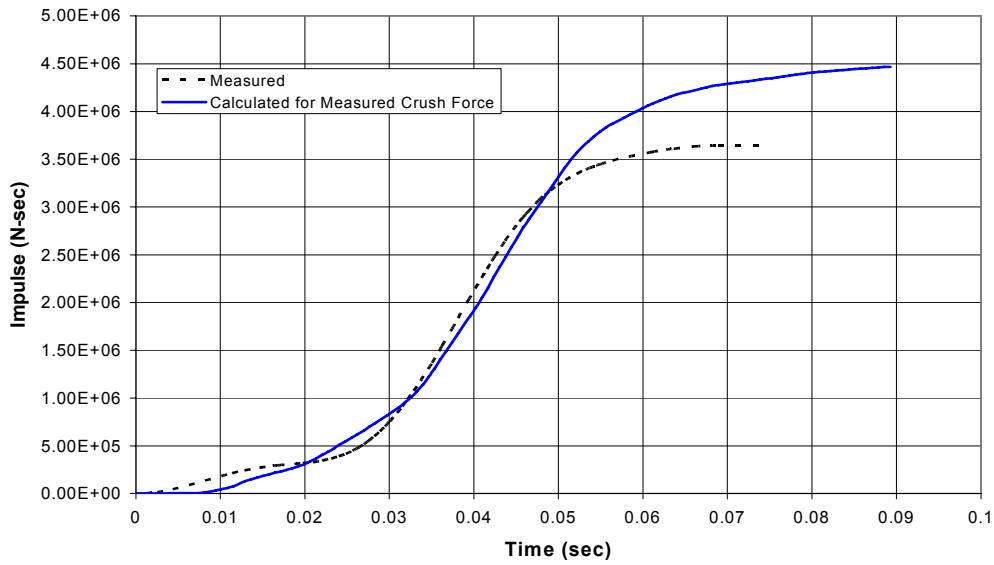
3-4

Figure 3-5. Comparison of Measured (Sugano, et al., 1993) and Calculated Impulse for the F-4 Aircraft Including Skids and Rockets [1 N = 0.225 Lbf]
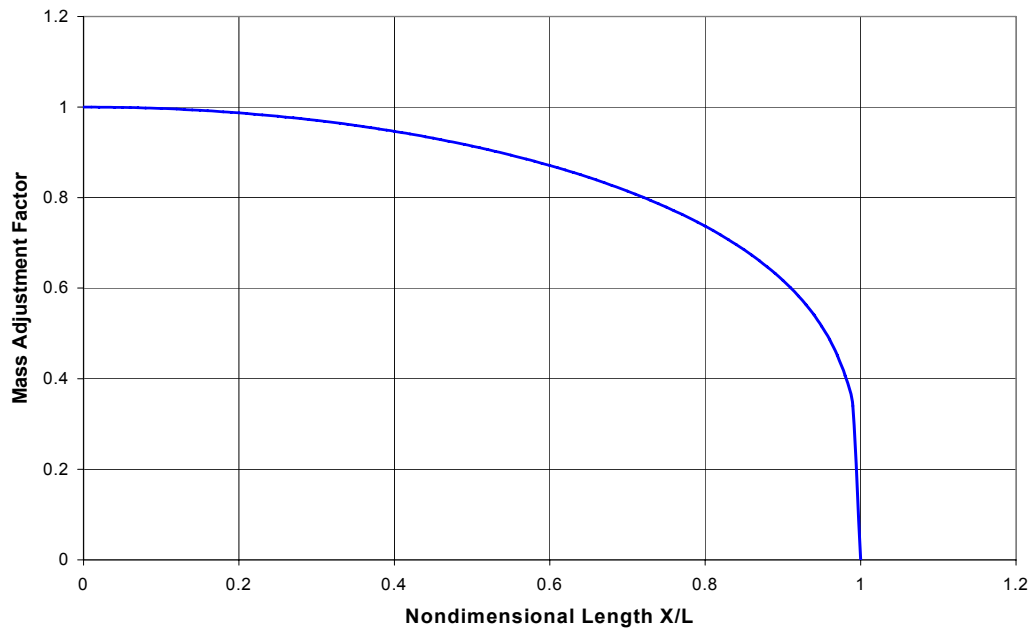
Figure 3-6. Proposed Nonlinear Mass Adjustment Factor Used in Calculation of Impulse Force

Figure 3-7. Comparison of Calculated Impulse Using Mass Adjustment Factor to Measured Impulse (Sugano, et al., 1993) for the F-4 Aircraft Including Skids and Rockets [1 N = 0.225 Lbf]
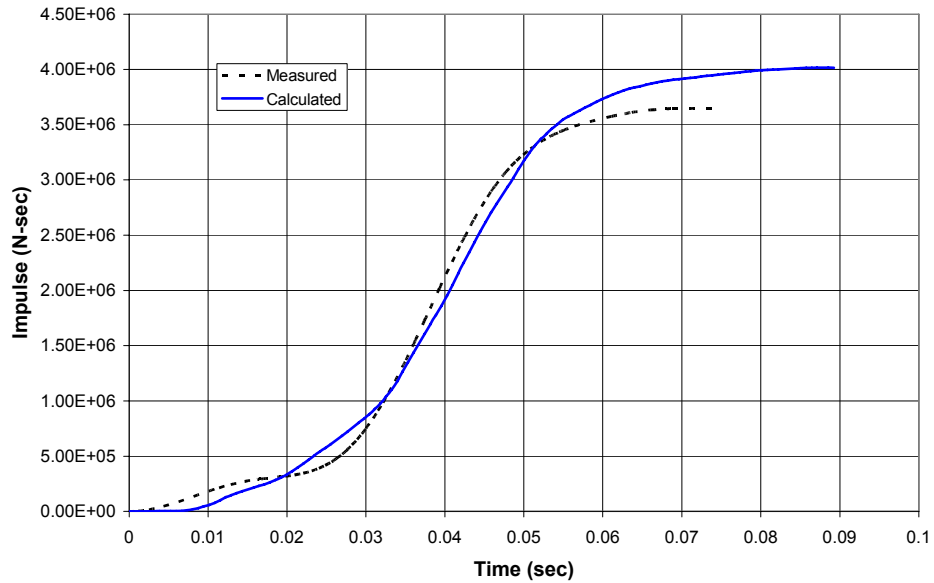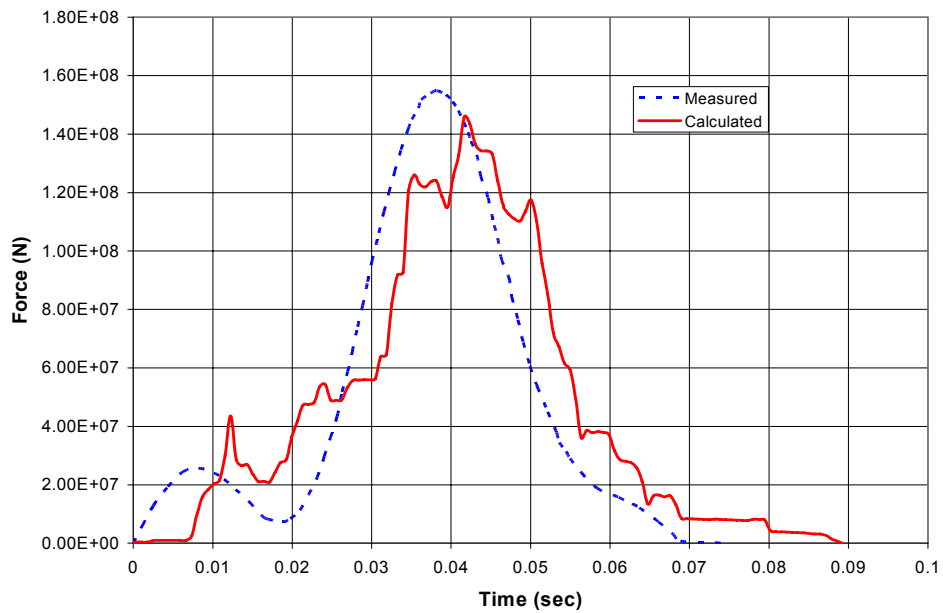

Figure 3-8. Comparison of Calculated Force Using Mass Adjustment Factor to the Measured Force (Sugano, et al., 1993) for the F-4 Aircraft with Skids and Rockets [1 m = 3.28 ft]

4 MODELING TARGET RESPONSE FOR THE FULL-SCALE F-4 IMPACT TEST

In this section, the global response of the large concrete block target due to the impact of a full-scale F-4 aircraft, as reported by Sugano, et al. (1993), is reproduced. In Sugano, et al. (1993), the goal of the experimental testing was to evaluate the overall force-time history resulting from the F-4 Phantom crashing into an essentially rigid wall (concrete block) at a velocity of 215 m/s [705.4 ft/s]. The concrete block rested on a concrete platform that incorporated air bearings to support the weight of the block and platform. In this report, numerical modeling to simulate the test consisted of creating and meshing a finite element model representing the large 7.0 × 7.0 × 3.66-m [22.9 × 22.9 × 12.0-ft] concrete block. Force-time loads from the actual measured load from the experiment and that using the Riera method are applied to study the block response and its comparison to test results.

4.1 Finite Element Model and Load Histories

The finite element model of the concrete block consisted of a mesh using 75,505 solid elements and used the concrete damage model of Section 2. A Flanagan-Belytschko viscous form with exact volume integration hourglass control solid element was used. The material parameters used in the concrete damage model are those previously listed in Table 2-3. The calculated mass of the block model was 468,960 kg [1,033,880 lb] as compared to the actual mass of 469,000 kg [1,033,968 lb]. Note that the concrete density was adjusted to more closely match the measured mass because the reinforcement steel was not defined by Sugano, et al. (1993) and was not included in the model. As reported by Sugano, et al. (1993), damage to the concrete block produced by the impact of the F-4 aircraft was limited to front face erosion. Also, because of the block thickness {3.66 m [12.01 ft]}, flexure and shear will not be significant response modes; thus, modeling the concrete block without rebar will be adequate for predicting back surface motions. The use of air bearings provided for an essentially frictionless contact between the bottom of the platform and the surface that it rested on (Sugano, et al., 1993). The air bearings and platform were not considered in the finite element model; instead, a frictionless interface was modeled between the base of the block and the ground plane.

The concrete block loading was defined by specifying a force-time history distributed over the impact area. The full-scale test results determined the estimated impact area was 10 m^2 [107.6 ft^2]. The idealized shape of the loading area used in the finite element model was a circle with its center at the center of the block. The force-time history was applied evenly over the circular area to each of the 647 nodes encompassed by the area. The results of the numerical modeling were compared with the available test data which measured the displacement and velocity at the center of the backside of the concrete block.

4.2 Load Histories: Experimental Data and the Riera Method

The first approach for specifying the load history used the actual measured load from the F-4 impact test which includes the sled and rockets used to accelerate the aircraft. The digitized force-time history used for the simulation is shown in Figure 3-8 as the measured data. The block velocity predicted by the numerical model and that of the test data is shown in Figure 4-1. Good agreement in the maximum velocity is observed between the data from the
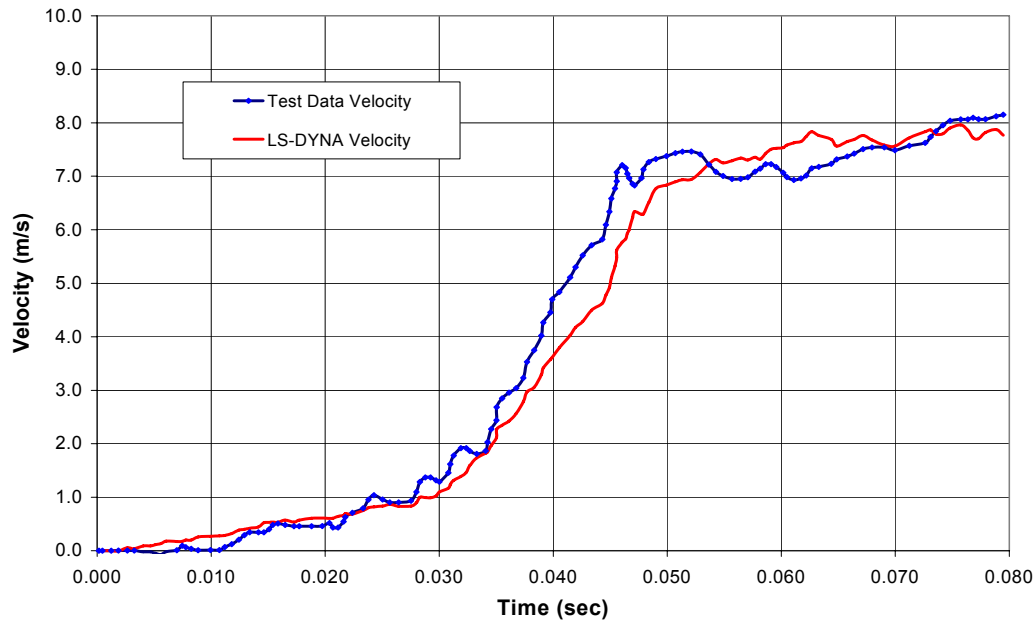
Figure 4-1. Comparison of LS-DYNA Calculated Target Block Velocity to Measured Target Block Velocity (Using the Measured Load in Figure 3-4) of Sugano, et al. (1993) [1 m = 3.28 ft]

test and the numerical results. A comparison of the displacements, measured on the back face of the target for the test and the numerical results, is shown in Figure 4-2.

In the test, a maximum penetration of 60 mm [2.36 in] was observed on the front face of the block and was partly a result of the engines impacting the block. However, the carriage sled and rockets caused the most significant damage (Sugano, et al., 1993). The numerical results did not show any penetration into the target. This was due to the loading method and relatively coarse mesh used for the numerical simulation. Note that a fine mesh was not used because the object of the analysis was not to capture the details of the penetration into the block, but rather to determine the overall global response of an essentially rigid structure. Also, because aircraft and sled loads were lumped together and applied over a large circular area, no local penetrations could be captured.

The second approach for the input load history of the F-4 and sled impact used the Riera method. The calculated load curve, using the Riera method shown in Figure 4-3, was applied to the concrete block model. A comparison of the velocity-time history of the numerical simulation versus the test data is shown in Figure 4-4. The numerical results show good overall agreement; however, the final velocity from LS-DYNA using the Riera method is approximately 7 percent higher than the test data velocity. These results tend to confirm the findings in Section 3 that the Riera method predicts loads that are conservative.

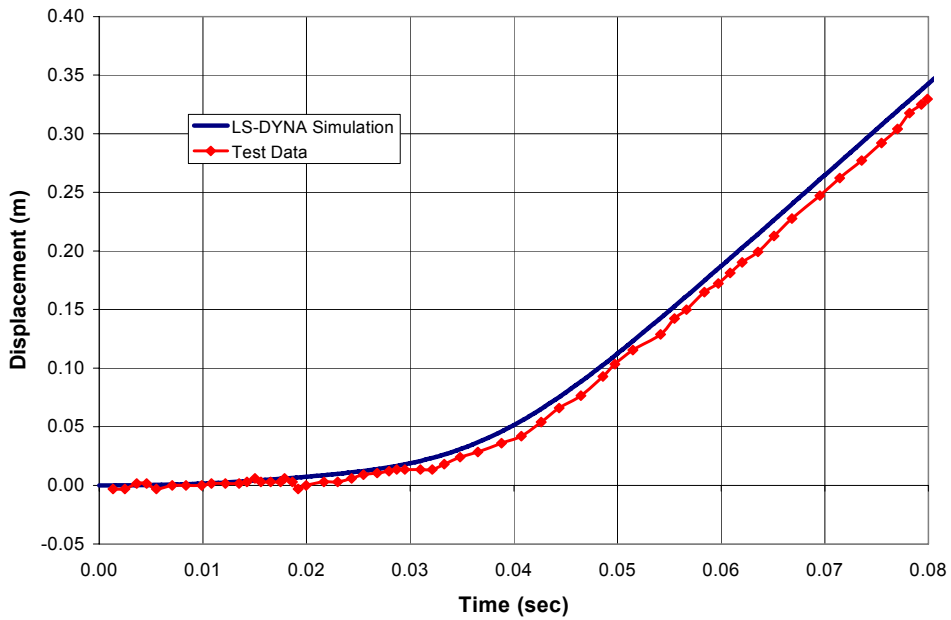**Figure 4-2. Comparison of LS-DYNA Calculated Displacement (Back Face of Target) Time History to Measured Test Data of Sugano, et al. (1993) [1 m = 3.28 ft]**
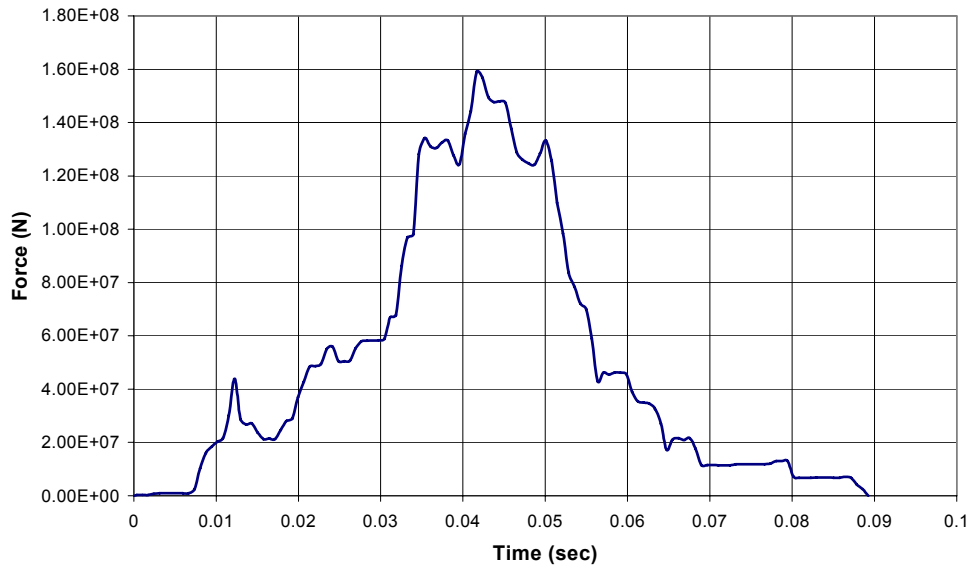

Figure 4-3. Calculated Load-Time History of the Full-Scale F-4 Aircraft Test Using the Riera Method (Riera, 1968) [1 N = 0.225 Lbf]
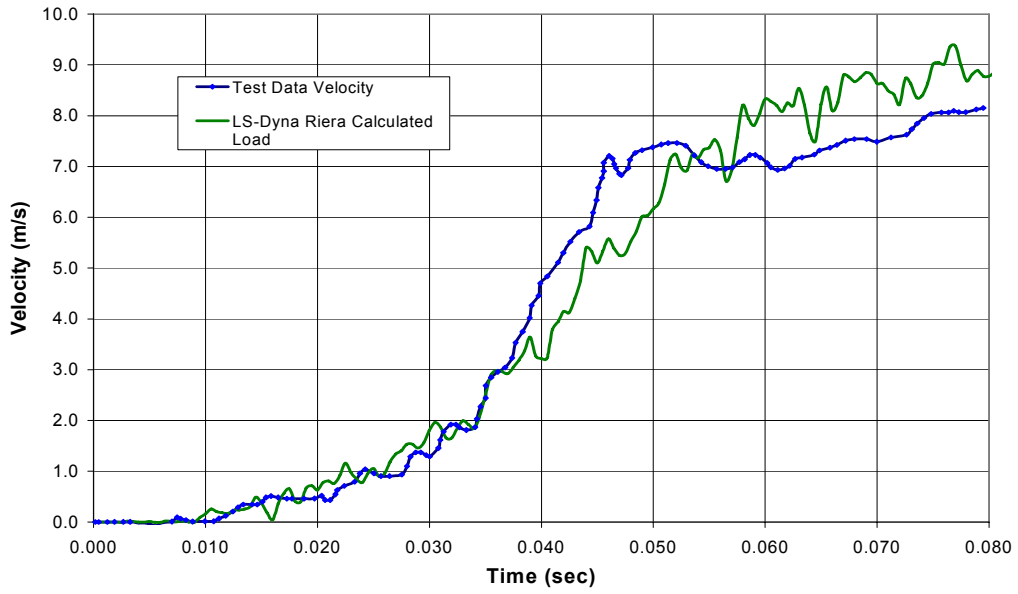
4-3

Figure 4-4. Comparison of Test Data (Sugano, et al., 1993) With Simulation Results Using the Riera-Derived Loading [1 m = 3.28 ft]

5 PRELIMINARY IMPACT STUDIES FOR A REINFORCED CONCRETE WALL

Based upon the work in Sections 3 and 4 of this report, a preliminary numerical simulation is presented for a reinforced concrete wall. Two views of the complete model showing the wall strike and rear faces are given in Figure 5-1. Again, the F-4 aircraft has been chosen since it is comparable in weight to an F-16. The F-4 aircraft has a gross weight of approximately 18,127 kg [40,000 lb] and is assumed to impact the wall at a speed of 190 m/s [623 ft/s]. This speed was selected so the wall was able to stop perforation due to the load. A time-varying load of the F-4, as determined using the Riera method (Riera, 1968), is shown in Figure 5-2 and will be applied to the finite element model.

5.1   The Finite Element Model

The wall was modeled as a 47.9-m [157-ft]-long, 19.5-m [64-ft]-high, and 1.4-m [4.5-ft]-thick section made of reinforced concrete. The wall is reinforced with #9 horizontal and #11 vertical steel reinforcement bars with a center to center spacing of 300 mm [12 in] with a 150-mm [6-in]-thick concrete cover measured from the surface of the wall to the edge of the bar. The tensile and compressive strength of the reinforcement bars used is assumed to be 414 MPa [60 ksi] with a yield strain of 0.002 and failure strain of 12 percent. The steel is modeled with the elastic-plastic kinematic hardening material model, and the concrete was modeled using the concrete damage model. Both models were described in Section 2. The concrete had a compressive strength of 23.5 MPa [3.4 ksi], and based on this compressive strength, all additional input parameters for the concrete damage model were calculated following guidelines given in the LS-DYNA Keywords User's Manual (Livermore Software Technology Corporation, 2003).

A total of 1,227,637 single-integration point solid elements were used to model the concrete portion of the wall with 15 solid elements used through the thickness. The steel reinforcement was modeled using beam elements. For the solid elements, a Flanagan-Belytschko viscous form with exact volume integration hourglass control was used. A fixed boundary condition was applied in the direction of loading for the top and bottom of the wall. Interior intersecting walls also were restrained in the direction of loading. A failure criteria for the concrete elements was applied using a strain erosion algorithm available in LS-DYNA (i.e., *MAT_ADD_EROSION) (Livermore Software Technology Corporation, 2003). This strain algorithm simulated concrete breakup associated with scabbing and spalling. A parametric study performed by Cox, et al. (2005) selected a strain erosion parameter of 0.5 based upon comparison with experimental results. The time-varying load, determined using the Riera method (Riera, 1968), is shown in Figure 5-2. This load was applied at the center of the wall over an area of 10 m^2 [108 ft^2]. In the finite element model, this area contains 1,460 nodes with the load divided equally at each node.

5.2   Finite Element Analysis of the Reinforced Concrete Wall

Results from the numerical simulation show a maximum displacement of about 0.54 m [24.25 in] at the center of the wall. The displacement-time history of a node located on the back side of the wall at the center of the impact area is shown in Figure 5-3. Note the oscillation in the wall displacement which shows the bounce-back response of the wall. Results of the numerical simulation also indicate tensile failure occurring at the back side of the wall.
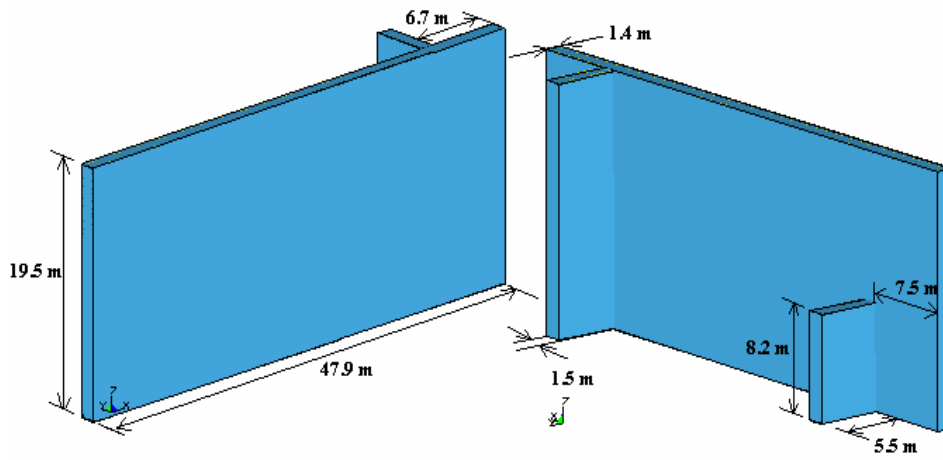
Figure 5-1. LS-DYNA Model of a Reinforced Concrete Wall Structure. Both Front and Rear View Shown [1 m = 3.28 ft].
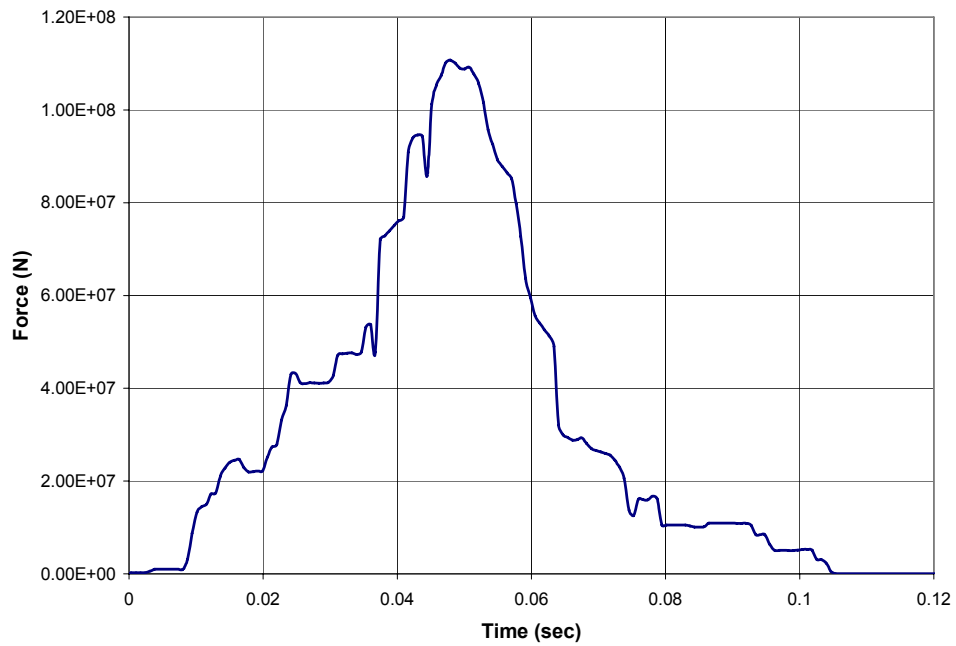

Figure 5-2. Calculated Load-Time History of F-4 at 190 m/s Using Riera Method [1 N = 0.225 Lbf]
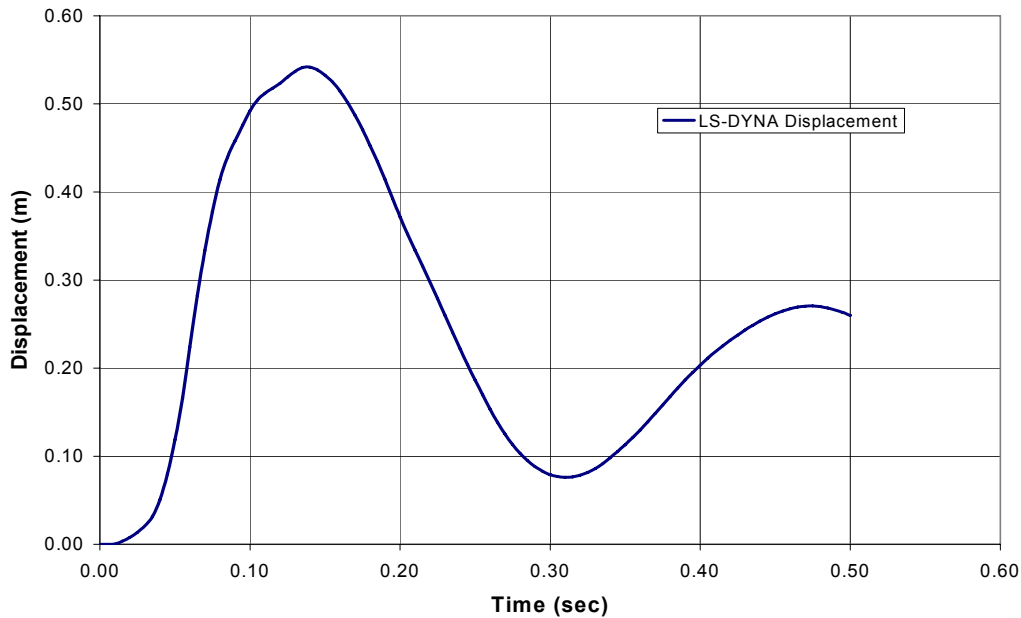
Figure 5-3. Displacement-Time History of a Node Located at the Center of the Back Side of the Wall [1 m = 3.28 ft]

This is evident from contours of plastic strain on the rear side of the wall at peak deflection. Cracking is likely to occur within the regions of high plastic strain indicated in Figure 5-4. Scabbing and spalling on the rear side of the wall was evident in the numerical simulation. This was derived from the observation that some elements were eroded (i.e., deleted) in the numerical simulation by the strain erosion algorithm. A view of plastic strain contours at maximum deflection on the back side of the wall is shown in Figure 5-4.

Contours of effective stress and plastic strain at maximum deflection are also shown on the front side of the wall in Figure 5-5. The contours of plastic strain on the front and back of the wall are similar in the region surrounding the loaded region. Examining cross sections through the wall in this region showed high strains on 45° planes through the wall with some elements deleted by the erosion criteria (50 percent strain). It appears that the wall had close to complete shear failure around the central loaded area, even though no perforation was evident. It is apparent that the wall was able to just stop perforation using the current loading methodology. It should be noted that the loading was applied over a relatively large area which assumes the load from the engines in particular is distributed evenly over the entire area. In reality, this is not the case, as shown from the full-scale engine simulant impact investigation (Sugano, et al., 1989) and as discussed in Section 4. Further investigation would require modeling the local damage caused by engine impact in addition to the global loading resulting from the entire aircraft structure.
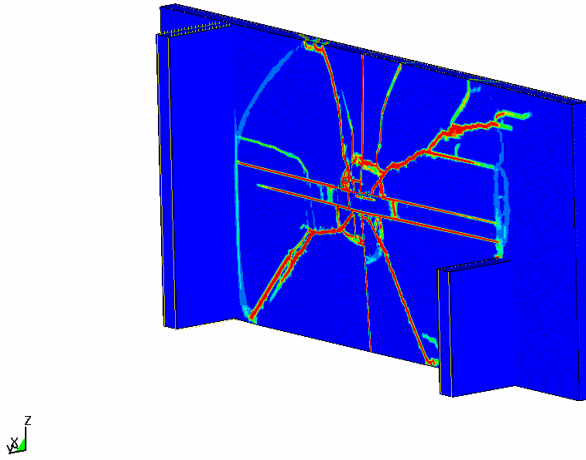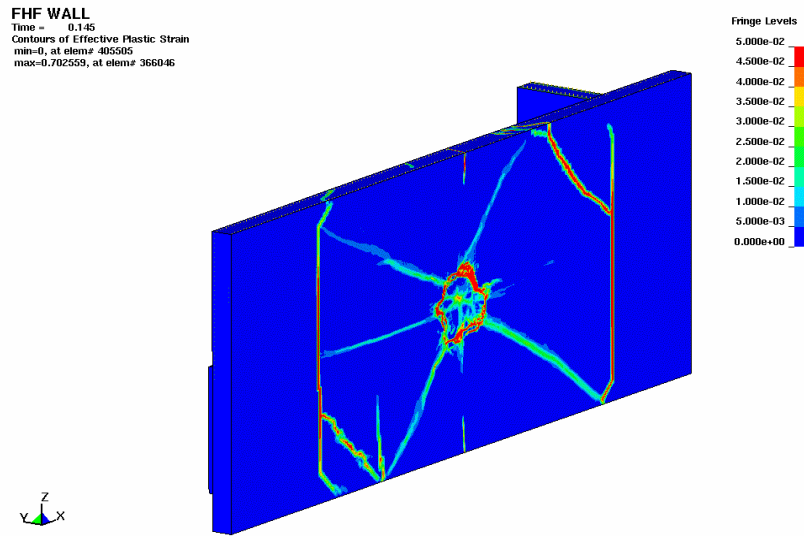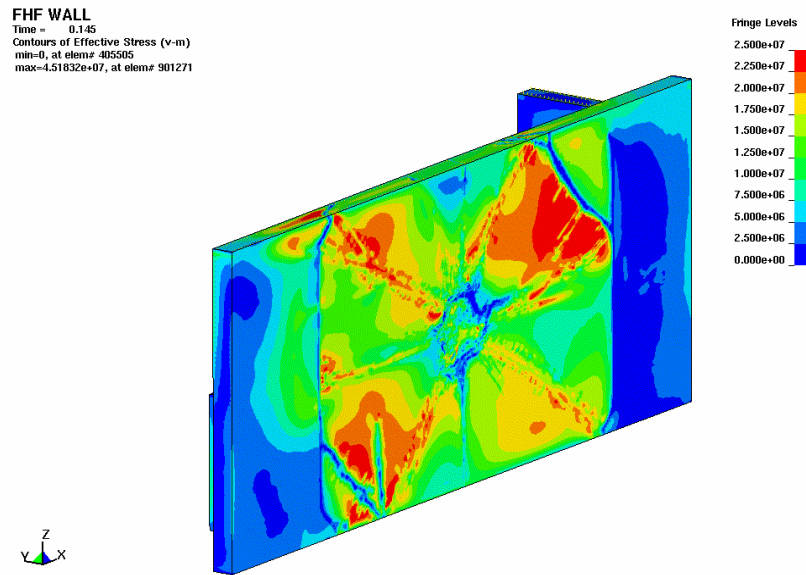
Figure 5-4. View of Plastic Strain Contours on the Back Side of the Reinforced Concrete Wall

(a)

(b)

Figure 5-5. Contours of (a) Plastic Strain and (b) Effective Stress (Pa) on the Front of the Reinforced Concrete Wall [1 Pa = 0.000145 psi]

6 SUMMARY AND CONCLUSIONS

This report documents the finite element modeling of the engine simulant used in full-scale tests as well as the structural response of the concrete wall target. Previous simulations performed for blast loading and missile impact for reinforced concrete walls have shown good agreement with available test data (Cox, et al., 2005).

One objective of this report was to improve the modeling capabilities required to simulate full-scale impact tests. This involved the modeling and analysis of the engine simulant and the behavior of the reinforced concrete. Results show that the present engine simulant finite element model behaves similarly, in terms of load displacement and absorbed energy, to the full-scale idealized engine when subjected to a quasi-static crush test.

The NRC requested that the concrete damage model be modified to improve correlation with the full-scale impact experiment. It has been shown that minor changes to the damage parameters improved correlation with the wall back surface displacements measured in the full-scale engine model test. Specifically, the structural response in the form of bounce back in the wall displacement was predicted with the results generally showing qualitative agreement. Most importantly, this damage parameter adjustment produced only minor, consistent changes in front face penetration. Correlations between LS-DYNA simulations and test data give confidence in material parameter selection and that the concrete damage model in LS-DYNA can be used effectively to model both localized and large-scale damage to reinforced concrete structures produced by impact loading. With the results of this and the previous (Cox, et al., 2005) studies, the input parameters used for the numerical concrete damage model in LS-DYNA have been verified for a range of applications.

A second objective was to study the Riera method, which computes the loads imparted to a rigid surface by an aircraft crash. Results compare favorably to measured loads reported in the literature (Sugano, et al., 1993). Preliminary analyses also have been conducted to evaluate impact damage produced by the F-4 aircraft comparable in size to the F-16 and with weight distribution data (required for the Riera method) available in the open literature. A simulated, reinforced concrete wall was modeled using the Riera method to calculate the impact force. The numerical simulation indicated tensile failure occurring at the back side of the wall based upon contours of plastic strain. At peak deflection, these tensile stresses indicated that cracking is likely to occur with scabbing and spalling on the rear side of the wall. Results obtained from these simulations appear to be reasonable; however, since the loading was applied over a relatively large area, additional modeling is required to capture local effects.

This study has demonstrated (i) the adequacy of the engine simulant finite element model and (ii) the appropriate selection of material parameters to characterize the response of reinforced concrete structures under impact loading. Correlation of numerical simulation results with experimental observations allowed the selection of the appropriate material damage models for concrete under impact loads. A methodology was established to determine the values of the concrete damage model parameters. Finally, the Riera method was used to compute loads on a structure imparted by an aircraft crash. It has been determined that the Riera method is conservative.

Staff will continue to verify and validate the software. This work does not come under the purview of safeguard analysis. Additional numerical studies regarding the adequacy of the modeling approach, the selection of material parameters to characterize the response of reinforced concrete structures under impact loading, and the methods of computing loads on structures impacted by an aircraft crash may continue. The selected concrete damage model and the associated material parameters may be used in the future to simulate the impact of different types of aircraft on reinforced concrete buildings. Future analyses may use characteristics of the actual structures under consideration and real threat (e.g., realistic models of the aircraft, realistic impact speed, etc.) and will be conducted in the future under safeguard restrictions.

7 REFERENCES

Ashley, K.L. "Identification of Aircraft Hazards." 000–30R–WHS0–00100–000–005. Bechtel SAIC Company, LLC. Las Vegas, Nevada: March 2005.

Cox, P.A., J. Mathis, and A. Ghosh. "Assessment of Structural Robustness Against Aircraft Impact At The Potential Repository At Yucca Mountain—Progress Report." San Antonio, Texas: CNWRA. August 2005.

Esashi, Y., Y.H. Ohnuma, C. Ito, and K. Shari. Experimental Studies on Local Damage of Reinforced Concrete Structures by the Impact of Deformable Missiles, Part 2: Intermediate-Scale Tests. Transaction of the 10th International Conference on Structural Mechanics in Reactor Technology (SMiRT 10). Los Angeles, California: American Association for Structural Mechanics in Nuclear Reactors. August 14–19, 1989.

Flanagan, D.P. and T. Belytschko. "A Uniform Strain Hexahedron and Quadrilateral and Orthogonal Hourglass Control." International Journal of Numerical Methods in Engineering, Vol 17. pp. 679–706. 1981.

Kokajko, L.E. "Department of Energy Preliminary Revision of Frequency Analysis of Aircraft Hazards for License Application." Letter from L.E. Kokajko to Mark H. Williams, Director, Office of License Application and Strategy. U.S. Department of Energy. Washington, DC: NRC. January 6, 2006. (ADAMS document accession number ML053530147.)

Livermore Software Technology Corporation. "LS-DYNA Keyword User's Manual." Version 970. Livermore, California: Livermore Software Technology Corporation. April 2003.

Malvar, L.J., J. Crawford, J. Wesevich, and D. Simons. "A Plasticity Concrete Material Model for DYNA3D." International Journal of Impact Engineering. Vol. 19, Nos. 9–10. pp. 847–873. 1997.

Microsoft Corporation. "Microsoft Excel 2002.5P3." Redmond, Washington: Microsoft Corporation. 2002.

Morissette, R.P. and J.A. Ziegler. "Identification of Aircraft Hazards." TDR–WHS–RL–000001, Rev. 00. Las Vegas, Nevada: Bechtel SAIC Company, LLC. June 2002.

Muto, K., H. Tackihawa, T. Sugano, H. Tsupota, N. Nagamatsu, N. Koskika, M. Okano, K. Juzuki, and S. Orui. "Experimental Studies on Local Damage of Reinforced Concrete Structures by the Impact of Deformable Missiles, Part 3: Full-Scale Tests." Transaction of the 10th International Conference on Structural Mechanics in Reactor Technology (SMiRT 10). Los Angeles, California: American Association For Structural Mechanics in Nuclear Reactors. August 14–19, 1989.

Ragan, G.E. "Frequency Analysis of Aircraft Hazards for License Application."
000–00C–WHS0–00200–000–00C. Las Vegas, Nevada: Office of Civilian Radioactive Waste
Management. Department of Energy. May 2005a.

Ragan, G.E. "Frequency Analysis of Aircraft Hazards for License Application."
000–00C–WHS0–00200–000–00D. Las Vegas, Nevada: Office of Civilian Radioactive Waste
Management. Department of Energy. May 2005b.

Ragan, G.E. "Frequency Analysis of Aircraft Hazards for License Application."
CAL–WHS–RL–000001. Rev. 00B. Las Vegas, Nevada. Office of Civilian Radioactive Waste
Management. Department of Energy. June 2003.

Reamer, C.V. and A.V. Gil. "Summary Highlights of NRC/DOE Technical Exchange and
Management Meeting on Pre-Closure Safety." Las Vegas, Nevada. July 24-26, 2001.

Riera, J.D. "On the Stress Analysis of Structures Subjected to Aircraft Crash on Building
Structures." Amsterdam, Holland: Nuclear Engineering and Design, North Holland Publishing
Company. pp. 415–426. 1968.

Sugano, T., H. Tsubota, Y. Kasai, N. Koshika, S. Orui, W.A. von Riesemann, D.C. Bickel, and
M.B. Parks. "Full-Scale Aircraft Impact Test for Evaluation of Impact Force." Nuclear
Engineering and Design 140. pp. 373–385. 1993.